Numerical modelling and sensitivity analysis of natural draft cooling towers

A. Dhorat [1], M. A. Al-Obaidi [1, 2] and I.M. Mujtaba [1, *]

[1] School of Engineering, Faculty of Engineering and Informatics. University of Bradford. Bradford, West Yorkshire BD7 1DP, UK
[2] Middle Technical University, Iraq – Baghdad
***Corresponding author, Tel.: +44 0 1274 233645**
E-mail address: I.M.Mujtaba@bradford.ac.uk

Abstract

Cooling towers are a relatively inexpensive and consistent method of ejecting heat from several industries such as thermal power plants, refineries, and food processing. In this research, an earlier model from literature was to be validated across three different case studies. Unlike previous models, this model considers the height of the fill as the discretised domain, which produces results that give it in a distribution form along the height of the tower. As there are limitations with the software used (gPROMS) where differential equations with respect to independent variables in the numerator and denominator cannot be solved, a derivative of the saturation vapour pressure with respect to the temperature of the air was presented. Results shown were in agreement with the literature and a parametric sensitivity analysis of the cooling tower design and operating parameters were undertaken. In this work the height of fill, mass flowrates of water and air were studied with respect to sensitivity analysis. Results had shown large variations in the outlet temperatures of the water and air if the mass flows of water and air were significantly reduced. However, upon high values of either variable had shown only small gains in the rejection of heat from the water stream. With respect to the height of the fill, at larger heights of the fill, the outlet water temperature had reduced significantly. From a cost perspective, it was found that a change in the water flowrate had incurred the largest cost penalty with a 1% increase in flowrate had increased the average operating cost by 1.2%. In comparison, a change in air flowrate where a 1% increase in flowrate had yielded an average of 0.4% increase in operating cost.

Keywords: Cooling Towers; Numerical Modelling; Sensitivity Analysis; Mass Transfer; Cost Analysis

1. Introduction

Counterflow cooling towers are being extensively used to cool industrial heated water by rejecting heat to the atmosphere of several industries including petroleum refineries, nuclear power plants, chemical industries, and coal power plants.

A cooling tower works by the principle of evaporative cooling whereby a medium to be cooled such as water is sprayed from the top of the tower over a heat transfer medium called the "fill". It is the fill, which disperses the water into thin films or droplets in order to maximise surface area so that sensible heat transfer and evaporative cooling is maximised. Therefore, it can be said that the mass and heat transfer performance is positively proportional to water-air interfacial contact area and heat transfer coefficient. For clean water applications, a film fill is ideal owing to its ability to maximise the surface area (Verma, 2004). However, for dirty water applications where the possibility of fouling is to be high, a splash type fill would be suitable as the water would be in the form of droplets in which the foulants would be entrained. Ambient air is then passed through the bottom of the tower and is in contact with the film of air in order to induce the evaporation of water through mass transfer. Figure 1 shows a schematic diagram of a natural draft wet-cooling tower and its interior parts. Figure 2 shows the cooling process at the air-water interface.

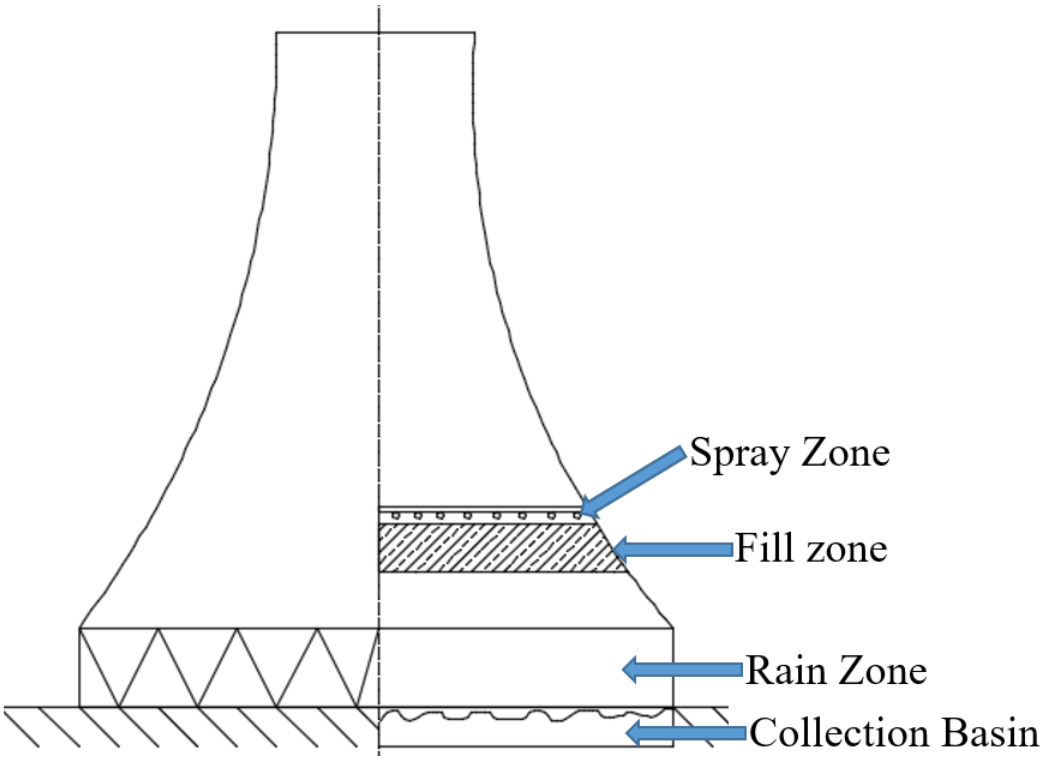

Figure 1. Schematic diagram of a natural draft cooling tower

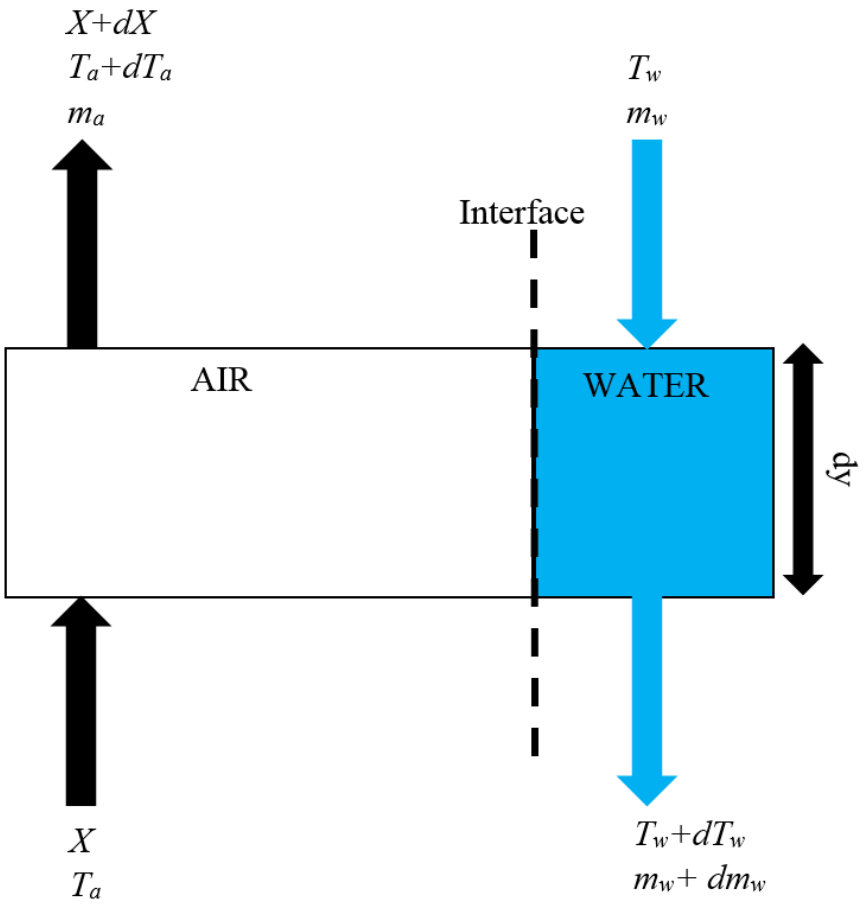

Figure 2. Depiction of cooling process at the interface

Various types of models have been proposed to elucidate the mass and heat transfer phenomena in the counterflow cooling tower based on different limitations. The earliest model found in open literature regarding modelling of a cooling tower was developed by Merkel (1925) of sets of differential equations, which incorporates mass and energy equations. However, as the original literature is in German, the main assumptions of the model were mentioned by Jin et al. (2007) and Kloppers and Kroger (2004). Key assumptions of the model were; a) Water loss due to evaporation was neglected in the energy balance. b) The Lewis factor was assumed to be unity. c) Specific heats of air-water mixture were assumed constant throughout the tower. d) Air leaving the cooling tower is saturated with water vapour and will be characterised by the enthalpy differential. The Merkel method of modelling the cooling tower is shown in Eq. (1). The meaning of the Merkel number is that it is an approximation of heat load being ejected into the air stream by the difference in the enthalpy of the air stream at the surface of the water and the enthalpy within the actual stream of air. The actual performance required by the cooling tower is the inverse of this difference as shown in Eq. (1).

$$Me_M = \int_{T_{wo}}^{T_{wi}} \frac{c_{pw} dT_w}{(i_{masw} - i_{ma})} \quad (1)$$

However, Eq. (1) is not self-sufficient and therefore an energy balance must be utilised for a numerical solution as shown in Eq. (2).

$$m_w c_{pwm} dT_w = m_a di_{ma} \quad (2)$$

Having said this, it is found in literature that Merkel's approach was not correct due to his oversimplifications within the model. For example, it has been shown by Feltzin and Benton (1991) that assuming a Lewis factor of unity is not correct as a Lewis number of 1.25 is more accurate.

Jaber and Webb (1989), proposed an alternative model of a cooling tower whilst utilising the same assumptions used for the Merkel model. The governing equation can be found below:

$$e = \frac{Q}{Q_{max}} = \frac{m_w c_{pw}(T_{wi} - T_{wo})}{C_{min}(i_{masw} - \lambda - i_{mai})} \quad (3)$$

Where λ is the correction factor as shown by Berman (1961). The number of transfer units are expressed as:

$$NTU = \frac{1}{1-C} ln \frac{1-eC}{1-e} \quad (4)$$

As the e-NTU model uses the same assumptions as the Merkel model, it is said the results of both models are very similar (Hajidavalloo et al., 2010). Furthermore, the limitations of the model are also the same as those found for the Merkel model.

Poppe and Rogener (1991) proposed an extended form of the original Merkel equation where the governing equations are shown below:

$$\frac{Me_p}{dT_w} = \frac{c_{pw}}{i_{masw} - i_{ma} + (Le_f - 1)[i_{masw} - i_{ma} - (w_{sw} - w) i_v] - (w_{sw} - w) c_{pw} T_w} \quad (5)$$

$$\frac{m_w}{m_a} = \frac{m_{wi}}{m_a} \left(1 - \frac{m_a}{m_{wi}} (w_o - w) \right) \quad (6)$$

According to Kloppers and Kroger (2005a) who undertook a study to investigate the differences between the Poppe and Merkel methods. The results of the study showed that below 26 ℃, the temperature outputs of both models will be in agreement. However, above 26 ℃ the outlet temperatures vary significantly due to the fact that the Lewis number will change significantly. The study also showed that as the Poppe method is the more rigorous method due to a greater of unknowns considered, as well as the change in the degree of saturation of air, it is a much better model to use in order to predict the path of cooling on a psychrometric chart.

Khan et al. (2003) generated a detailed mathematical model of a counter flow wet cooling tower to investigate the performance characteristics. It was found that the predominant mode

of heat transfer was evaporation. 62.5% of the heat transfer at the bottom of the tower was due to evaporation and 90% of the heat transfer at the top was due to evaporation.

Kloppers (2003) outlined a critical analysis of the Merkel, e-NTU and Poppe methods. Moreover, he developed a detailed computer program for prediction and optimisation of cooling towers. Then, he addressed the limitations of all three models by extending an empirical relationship for the loss coefficient of fills through accounting for viscous and drag effects. Further refinement of the model included accounting for buoyancy, momentum, and fill height effects.

Kloppers and Kroger (2005b) illustrated a detailed derivation of modelling a counterflow wet cooling tower from first principles, which later led to the Poppe model. The governing equations of the Poppe model were extended to create a detailed representation of the Merkel number.

Yang et al. (2007) utilised a finite element method to calculate the flow fields in a natural draft cooling tower and a two-dimensional (length and time) model was proposed. It was found in the numerical solution that the internal pressure had risen when the tower altitude increased. In addition, it was noted that the heat transfer is the highest in the centre of the column as opposed to the walls.

Lemouari et al. (2009) carried out an experimental analysis of heat and mass transfer phenomena within a direct-contact cooling tower. In this study, two operating regimes were found; pellicular and bubble and dispersion regimes. The pellicular regime existed with low water flow rates and with higher flow rates, a bubble and dispersion regime was noted. The study concluded that at high inlet water flowrates (bubble and dispersion regime) had given better heat and mass transfer characteristics. However, this kind of behaviour is like to be specific to the VGA type packing and it cannot be said with certainty that the same principles can be applied to different types of packing.

Klimanek (2013) presented an extensive one-dimensional model based upon first principles so that the mass transfer coefficient in the z-axis could be determined. This one-dimensional model was then incorporated into a full 3D CFD model capable of predicting cooling tower performance under various operating conditions. Different flow patterns were observed within the 2D and 3D models; however, a limitation of his work was that the mass transfer coefficient was constant throughout the whole tower even though it was a 3D model.

Gao et al. (2013) developed an artificial neural network to research the effect of cross winds on the performance of a cooling tower. The input variables included; level Froude number, water spraying density, inlet water temperature and relative humidity of inlet air. The output

variables were cooling efficiency, heat transfer coefficient, mass transfer coefficient, temperature difference and evaporative loss proportion. Good statistical performance was found with a range of R to be in between (0.992-0.999). The limitations of the model were that it was nothing more than an empirical correlation for one specific type of tower; it would not have been possible to apply the neural network amongst a range of different towers.

Nasrabadi and Finn (2014) outlined a model, which focused on low approach temperatures (14 ℃ - 18 ℃). A "corrected" effectiveness NTU method was proposed which incorporated the change in mass flow due to evaporation as well as estimating the specific heat of air-stream mixture at each interval of the calculations. Compared to experimental data, the root mean square difference error of the water outlet temperature was found to be ± 1.32%. However, the limitations found in the in model was that the Lewis number was assumed to be 1 and only the air leaving the tower would be saturated.

Shah and Tailor (2015) presented the design procedure of counter flow cooling towers using the Merkel's method and a lab scale apparatus was fabricated. Results of the lab scale tower showed good agreement with the proposed optimised design of the tower.

Llano-Restrepo and Monsalve-Reyes (2017) undertook a thorough literature review on existing models available within open literature. Their literature review had shown that the works of Osterle (1991) was proven to be incorrect. The paper had also proposed a new model from first principles called a continuous differential air water contactor model (CDAWC). The key contribution of this model was that the heat and mass transfer coefficients were not lumped together but individually calculated and used in the model. The results of the proposed CDAWC model had shown good agreement with the results obtained from the model of Klimanek (2013). Limitations of the model is that it is only valid for when the fill is completely wetted, and only average specific heats were used.

Martin and Martin (2017) carried out a multi-period design of natural draft cooling towers whereby the impact of variable weather over the course of a year on a cooling tower was investigated. A nonlinear optimisation program was solved in order to obtain the optimum geometry required under variable weather. Results had shown that hotter climates consume around 5% more water and require nearly twice the heat transfer area compared to cooler climates. A limitation found in this study was that the mass transfer coefficient used in the work was not experimentally derived from an existing fill; rather an existing correlation from literature was used.

As the discussions outlined in this section has focused on the different types of modelling of cooling towers in the literature, it has been observed that with the exception of experiments, a

parametric sensitivity analysis of various factors using a distribution model has not yet been explored. Therefore, the objectives of this research are to initially recreate the simulations produced by Klimanek (2013) and cross validate the results with that of the paper as it lacks the thermophysical property correlations used by the author. As previous works have focused on induced draft cooling towers, this work will focus on natural draft cooling towers, which are predominantly used in industry for large mass flows. As natural draft cooling towers utilise no fans, the main variables of interest are the height of the fill, the mass flowrates of water and the mass flowrate of air. These variables will be used for a parametric sensitivity analysis using a base case study obtained from Klimanek (2013). The output variables under investigation are the outlet temperatures of water and air as well as the hourly operating cost along with pumping power. The main contribution of this work to the new body of knowledge is the quantification of sensitivity analysis on the power requirements and operating cost on the cooling towers. To the authors knowledge, no previous work has been undertaken on the operating cost analysis of natural draft cooling towers. One particular advantage of this research is in the design of cooling towers as sensitivity analysis is crucial for the design and operation of a cooling tower where an envelope of operating parameters is required.

2. Validation

2.1 Model proposition

The one-dimensional model proposed by Klimanek (2013) is used as the basis for this work. This model was selected on the basis that it has already been benchmarked and validated with existing literature. Furthermore, this model would be suitable for undertaking a study in the operating parameters of the cooling tower, as it is possible to find spatial distributions of several parameters. For the unsaturated case where the humidity ratio is smaller than the saturation humidity, Eqs. (7) – (11) apply. Eq. (7) is a reduced form of the mass balance whereby the mass of water is dependent on the humidity differential between the humidity of the air and the saturation humidity at the water temperature. Eq. (8) describes the change in the humidity of the air as a function of the humidity differential per unit mass of air. Eqs. (9) – (10) are the air and water temperature differential characterised as a function of the heat and mass transfer coefficients along with the temperature differential and the humidity ratio differential.

$$\frac{dm_w}{dz} = \beta a A_z (X_s^w - X) \tag{7}$$

$$\frac{dX}{dz} = \frac{\beta a A_z (X_s^w - X)}{m_a} \tag{8}$$

$$\frac{dT_a}{dz} = \beta a A_z \frac{\left[Le_f (T_w - T_a)(C_{pa}^a + C_{pv}^a X) + (C_{pv}^w T_w - C_{pv}^a T_a)(X_s^w - X)\right]}{m_a (C_{pa}^a + C_{pv}^a X)} \tag{9}$$

$$\frac{dT_w}{dz} = \beta a A_z \frac{\left[Le_f (T_w - T_a)(C_{pa}^a + C_{pv}^a X) + (r_0 + C_{pv}^w T_w - C_{pw}^w T_w)(X_s^w - X)\right]}{m_w C_{pw}^w} \tag{10}$$

$$Le_f = 0.866^{\frac{2}{3}} \times \frac{\left(\frac{X_s^w + 0.622}{X + 0.622} - 1\right)}{ln\left(\frac{X_s^w + 0.622}{X + 0.622}\right)} \tag{11}$$

In an evaporative process such as the use of the cooling towers, the Lewis factor (Le_f) is a dimensionless form of the rates of heat and mass transfer as shown in Eq. (12). However, the individual mass transfer coefficients are difficult to obtain and therefore a correlation proposed by Bosnjakovic (1965) is utilised as shown in Eq. (11).

$$Le_f = \frac{\alpha}{\beta (c_{pa}^a + X C_{pv}^a)} \tag{12}$$

As the air stream becomes more saturated with water vapour, the system would eventually reach a supersaturated state whereby the humidity ratio of the air exceeded the saturation humidity ratio. When this occurs, it induces a change in the physics of the system as the water vapour would reach a dew point and thus water would start to condense and release the latent heat of vaporisation. When this occurs, the air temperature would decrease. Furthermore, the Lewis factor would also change as shown in Eq. (13).

$$Le_f = \frac{\alpha}{\beta (c_{pa}^a + X_s^a C_{pv}^a + c_{pw}^a (X - X_s^a)} \tag{13}$$

For the case of supersaturation, the four governing equations would now take the form of the following:

$$\frac{dm_w}{dz} = \beta a A_z (X_s^w - X_s^a) \tag{14}$$

$$\frac{dX}{dz} = \frac{\beta a A_z (X_s^w - X_s^a)}{m_a} \tag{15}$$

$$\frac{dT_a}{dz} =$$

$$-\beta a A_z \frac{\left[C_{pa}^a Le_f (T_a - T_w) - X_s^w (r_0 + C_{pv}^w T_w) + C_{pw}^a \left(Le_f (T_a - T_w)(X - X_s^a) + T_a (X_s^w - X_s^a)\right) + X_s^a (r_0 + C_{pv}^a T_w) Le_f (T_a - T_w) + C_{pv}^w T_w\right]}{\left[C_{pa}^a + C_{pw}^a X + \frac{dX_s^a}{dT_a}(r_0 + C_{pv}^a T_a - C_{pw}^a T_a) + X_s^a (C_{pv}^a - C_{pw}^a)\right]}$$

(16)

$$\frac{dT_w}{dz} = \beta a A_z \frac{[(r_0 + C_{pv}^w T_w - C_{pw}^w T_w)(X_s^w - X_s^a) + Le_f (T_w - T_a)(C_{pa}^a + C_{pw}^a (X - X_s^a) + C_{pv}^a X_s^a]}{m_w C_{pw}^w} \quad (17)$$

$$Le_f = 0.866^{\frac{2}{3}} \times \frac{\left(\frac{X_s^w + 0.622}{X_s^a + 0.622} - 1\right)}{ln\left(\frac{X_s^w + 0.622}{X_s^a + 0.622}\right)} \quad (18)$$

All correlations for specific heats, saturation pressures and saturation humidities can be found in the Appendix A. It is observed in Eq. (16) that there is a differential variable in the form of $\frac{dX_s^a}{dT_a}$ where the derivative is with respect to the temperature of air. An issue which arises is that the gPROMS model builder (general Process Modelling System by Process Systems Enterprise Ltd, 2001) does not natively support a variable with respect to which the derivative is calculated. Possible solutions included series expansion or Newton's difference quotient. However, these solutions are far from trivial and require a lot of unnecessary work. A workaround was devised in the form of plotting a graph of the saturation humidity with the temperature of the air. A polynomial regression of the 7th order was undertaken within Matlab as shown in Figure 3. As the saturation pressure is dependent on the ambient pressure, regression analysis must be undertaken for any ambient pressure. In the case of atmospheric pressure, the following regression analysis is only valid for an ambient pressure of 101,325 Pa.

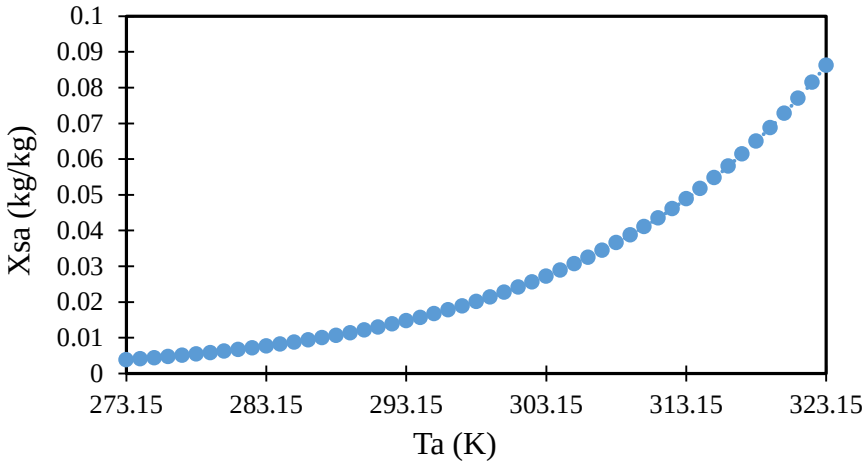

Figure 3. Linear regression of temperature of air and the saturation humidity of air at 101325 Pa

Linear regression of the two variables resulted in Eq. (19). R^2 was calculated be 1 which showed a perfect fit in comparison to the raw data.

$$X_s^a = (2.2521897129393E-14{T_a}^7) - (4.53959496755178E-11{T_a}^6) + (3.92594755437598E-08{T_a}^5) - (0.0001887926168040 72{T_a}^4) + (0.00545109732954153{T_a}^3) - (0.944891246126919{T_a}^2) + (91.0350445769598T_a) - 3760.30419558867 \quad (19)$$

Differentiating Eq. (19) yields the following:

$$\frac{dX_s^a}{dT_a} = 1.57653279905751E-13{T_a}^6 - 2.72375698053107E-10{T_a}^5 + 1.96297377718799E-07{T_a}^4 - 7.55170467216288E-05{T_a}^3 + 1.63532919886246E-02{T_a}^2 - 1.88978249225384T_a + 91.0350445769598 \quad (20)$$

As the volumetric mass transfer coefficient is dependent on the Merkel number, which is an empirically obtained value and varies along the height of the tower. A proposed method to obtain this value is to iteratively calculate the product of the volumetric mass transfer coefficient using Eq. (21). The left-hand side is calculated as a lumped parameter because A_z is assumed to be 1 and βa is known as the volumetric mass transfer coefficient.

$$\beta a A_z = Me \frac{m_{wi}}{H} \quad (21)$$

Once the value of the volumetric mass transfer coefficient ($\beta a A_z$) is obtained, it is possible to add it to the distribution model in the form of Eq. (22).

$$\frac{dMe}{dz} = \frac{\beta a A_z}{m_w} \quad (22)$$

2.2 Simulation Methodology

The simulation package of choice was gPROMS, which is an equation orientated custom modelling software. The governing equations were written with the "if" construct of when the humidity is saturated or not. Therefore, the software can check for saturation at every discrete point. The advantage of gPROMS is also the fact that it can handle partial differential equations as well as ordinary equations with inbuilt numerical solvers. This gives the advantage to the fact that models can be analysed under steady state and dynamic conditions. As the cooling tower is in a counter flow direction, it means that the water outlet parameters will have to be iteratively adjusted until the inlet conditions are met as shown in Figure 4. Compared to the solution strategy of Klimanek (2013), the software gPROMS does not

contain a shooting solver to solve two point boundary value problems. It is for this reason the iterative adjustment is required. Even though it holds longer computational times, the advantage of gPROMS is that the adaptive step size in the supersaturated state can be as small as 0.0000001, which would show different results to that of literature.

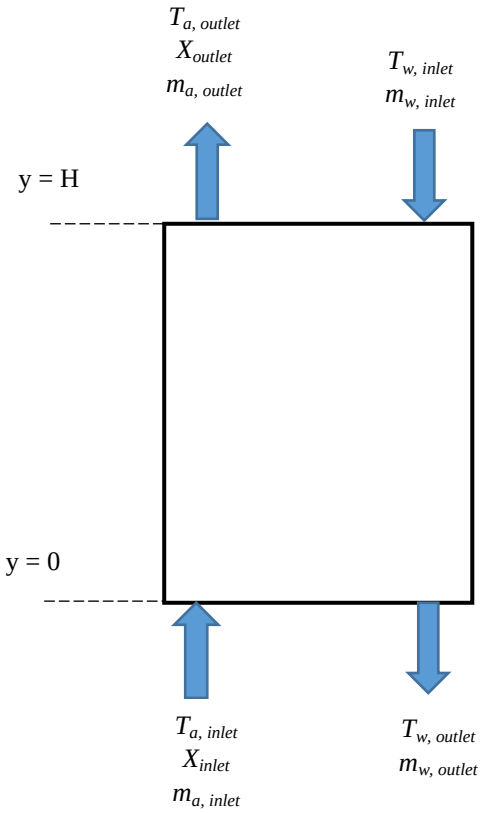

Figure 4. Schematic diagram of proposed distribution model

As the system of equations consist of ODE's and algebraic equations, the step integration of the height is undertaken with an inbuilt ODE solver called SRADU. It is a fully implicit Runge-Kutta method which implements a variable height step. The solver SRADU automatically adjusts the height step size without the need for user input as well as adjusting the integration order to maintain the error of integration within the allocated tolerance.

2.3 Validation of unsaturated air case study

As certain relationships used within the Klimanek (2013) model are not known such as specific heats and saturation humidity correlations, the model must be first computed and validated with the results of those from the literature. The first case study, which is used to validate the model, is the unsaturated case study as any discrepancies found would be due to the correlations used. The case data is found in Table 1.

Table 1. Input parameters for the unsaturated air case study

Parameter	Value
$m_{w,i}$	3.0 kg/s
m_a	3.0 kg/s
X_i	0.001 kg/kg
T_{wi}	37.0 ℃
T_{ai}	20.0 ℃
Me	1.8613
Height (fill)	1.2 m

Figure 5 shows that the temperature deviations of the air and water inlet in comparison to Klimanek (2013) was between 2–3 ℃. Therefore, the model has been validated, as the temperature difference of 3 ℃ is not significant enough to cause room for concern, as it is an engineering model. Due to the differences in solution methodologies as well using a new correlation for saturation pressure, small margins of error are acceptable. It is also observed that the air did not become supersaturated until near the end of the tower and the temperature difference between the water and the air was found to be positive throughout the tower. These results further validate the findings by Klimanek (2013) as it shows that the evaporation and convective heat transfer was positive.

In addition, the saturation humidity ratio and humidity ratio distributions within the tower were validated as results were in agreement with those of Klimanek (2013). As deviations were only found to be in the range of 0-5%, this would be down to the different water vapour saturation pressure equation used. Therefore, it is said that these results are deemed acceptable. Figure 6 shows these results.

Figure 7 shows the distribution of the Lewis factor over the height of the cooling tower. As these results were not discussed by Klimanek (2013), these results can only be compared to those of other literature. It can be seen that the Lewis factor ranges between 0.918 and 0.921, which is a significant demarcation from the assumptions of the Merkel model in which an assumption is made that the Lewis factor is unity throughout the tower. As the Lewis factor can dictate the rate at which heat is rejected from the cooling tower, such an assumption used by Merkel is not valid as if the Lewis factor was assumed to be constant at 1, the heat rejection rate would increase by ~9%. The decrease in the Lewis factor was expected as the

humidity ratio increased, and the saturation humidity evaluated at the water temperature decreased. However, the increase seen above 0.8 m was not expected. Possible reasons for this increase could be down to the fact that at 0.8 m the gradient of the humidity gradient looked to be constant. As the humidity gradient went towards being plateau, the saturation humidity evaluated at water temperature would relatively increase as the rate of heat ejected is increasing.

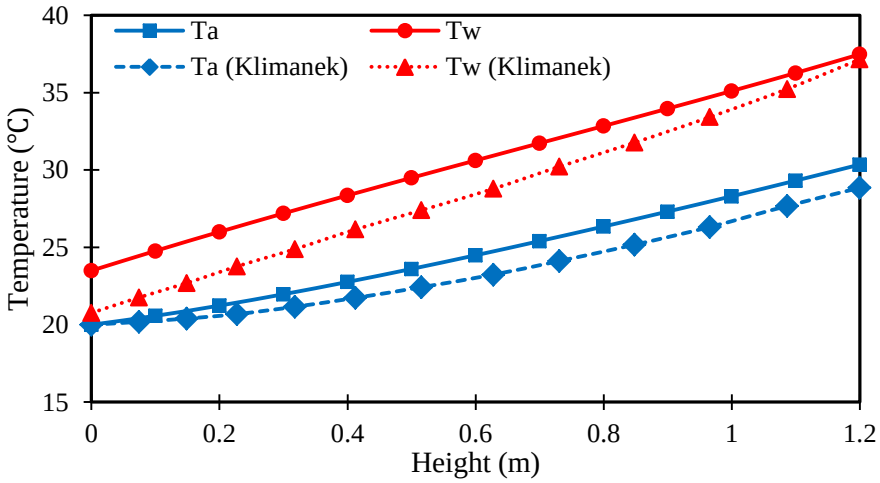

Figure 5. Temperature distribution results of unsaturated case

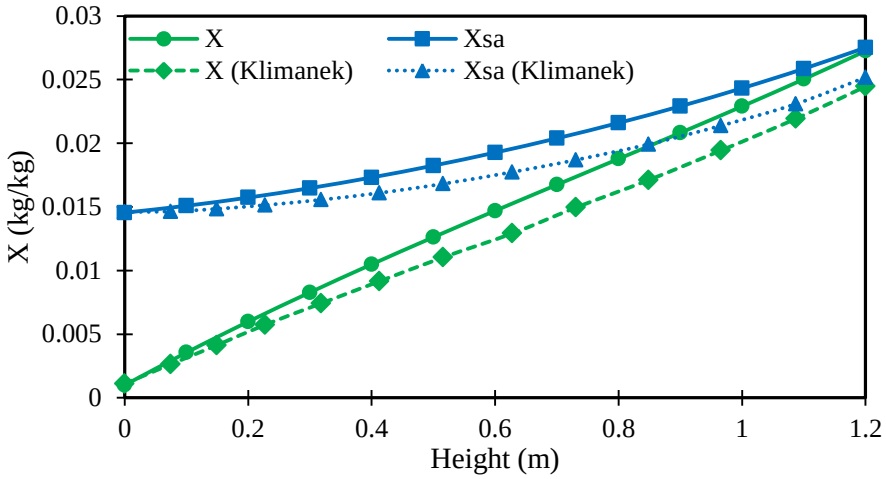

Figure 6. Humidity ratio distribution results of unsaturated case

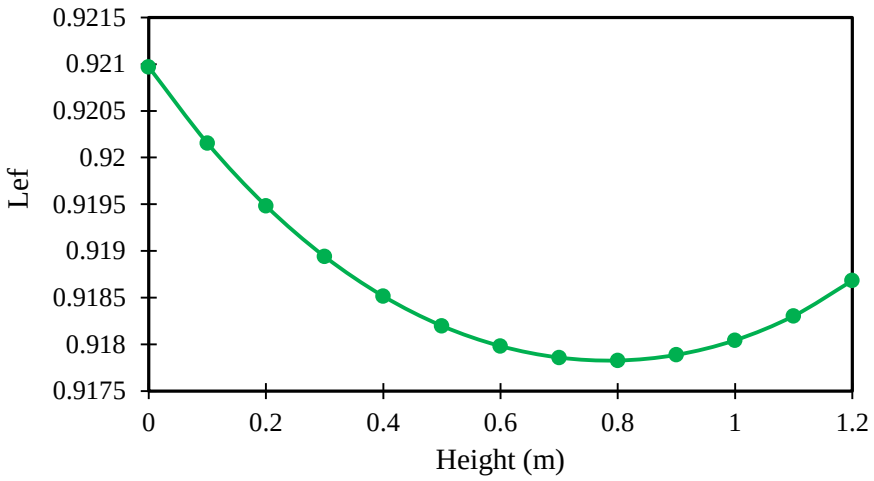

Figure 7. Lewis factor distribution results of unsaturated case

2.4 Validation of supersaturated air case study

As well as an unsaturated air case study, a saturated air case study was also needed to be validated before proceeding with the parametric sensitivity analysis. This study is critical due to many reasons as the saturated/supersaturated state can have significant implications on the heat rejection rate between the moist air and water streams. The initial conditions of the model are found in Table 2.

If supersaturation does occur in the model, it can be seen graphically when the humidity ratio and saturation humidity are plotted together. If the humidity ratio is higher than the saturation humidity, then supersaturation has occurred. As the equations in the supersaturated state become solved, the rate of air temperature heating up would decrease. As water is now condensing in the supersaturated state, the humidity ratio would begin to decrease it reaches the saturated state.

Table 2. Input parameters for the supersaturated air case study

Parameter	Value
$m_{w,i}$	3.0 kg/s
m_a	3.0 kg/s
X_i	0.012 kg/kg
T_{wi}	37.0 ℃
T_{ai}	20.0 ℃
Me	1.8613
Height (fill)	1.2 m

Results obtained from the simulation are shown in Figures 8 and 9. The temperature distributions obtained in Figure 8 are in agreement with the literature simulation results. It can be seen that after 0.54 m the system enters a saturated state where the gradient of the air temperature line changes. With respect to the outlet temperatures obtained for both water and air, the discrepancy found was only 1.75 ℃ and 1.11 ℃ respectively. Therefore, for the purposes of dynamic modelling, this steady state model can be used to build upon.

Analysis of the humidity distributions shows good agreement with literature values. However, as shown in Figure 9, the system does not become a supersaturated state as the humidity ratio becomes equal to the saturation humidity ratio. Whereas the literature simulation shows super saturation where water in the vapour stream condenses back into liquid. However, as the temperature and humidity distributions are similar, this is not a concern for the validity of the model. It could also be argued that these results are potentially more accurate as supersaturation is only a temporary state of which these results show as the system only reaches saturation.

The Lewis factor distribution can be seen in Figure 10 whereby the range was found to be between 0.915-0.916. Results were similar to those found in Section 2.3 whereby the Lewis factor would initially decrease before increasing. However, it was observed that in the simulation that the value at the top of the tower (0.9163) had a small increase in comparison to the bottom (0.9158). This is because in the saturated state, the water vapour is condensing back into the bulk liquid phase and as such, the rates of heat and mass transfer increase significantly.

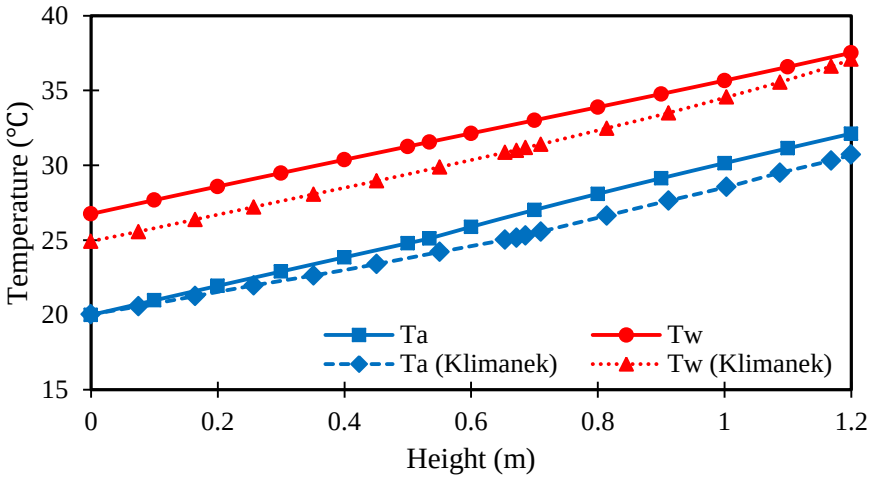

Figure 8. Temperature distribution results of supersaturated case

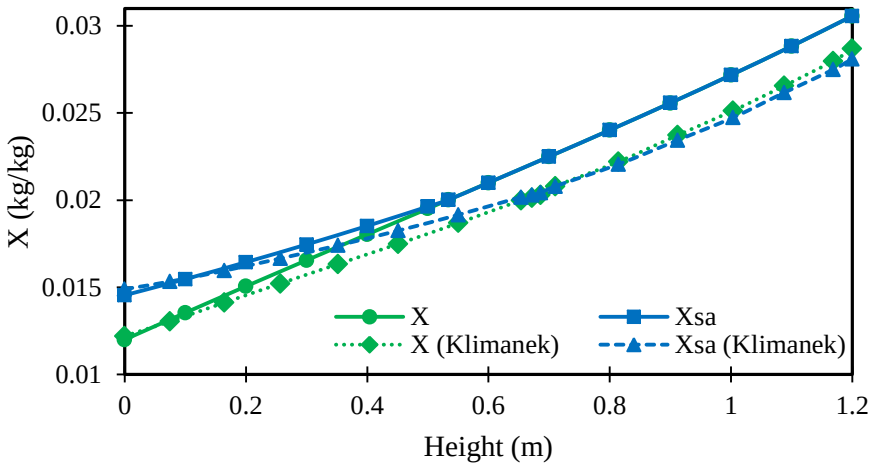

Figure 9. Humidity ratio distribution results of supersaturated case

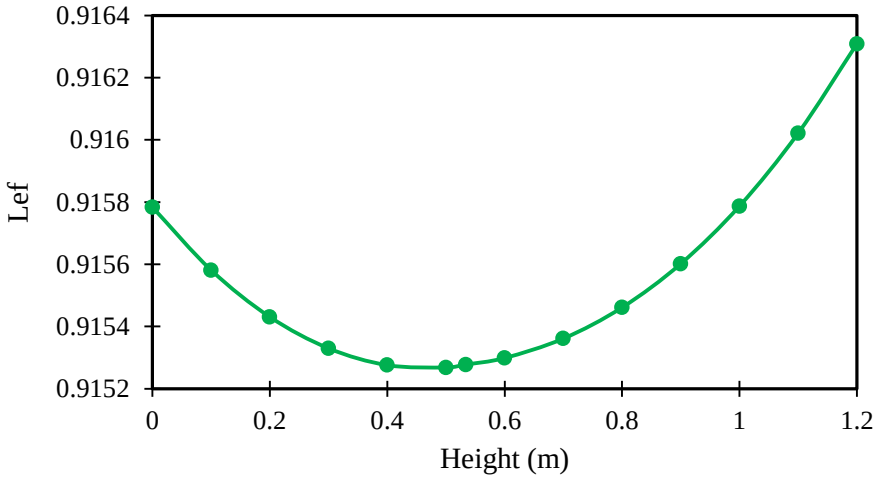

Figure 10. Lewis factor distribution results of supersaturated case

Results in Figures 11 and 12 show a small section of the results with a fine precision. With respect to the temperature distributions in Figure 11, it can be seen that there is only a small gradient increase in the temperature of air and a small gradient decrease in the temperature of water. However, it is the humidity ratio distribution in Figure 12, which is of the most interest as it shows that the value of the saturation humidity is not constant. Possible reasons for this behaviour is that when the supersaturated state occurs, water vapour would condense and heat up the water stream. By heating the water stream, the air stream would also heat up and thus the saturation humidity would increase, and the system would return to a saturated state. Another reason is due to the actual temperatures of both air and water streams increasing on such a small level so that cannot be seen in Figure 11, this may explain the small increases in the humidity ratio as in the saturated state, the water stream loses heat load as well as gaining heat from condensation.

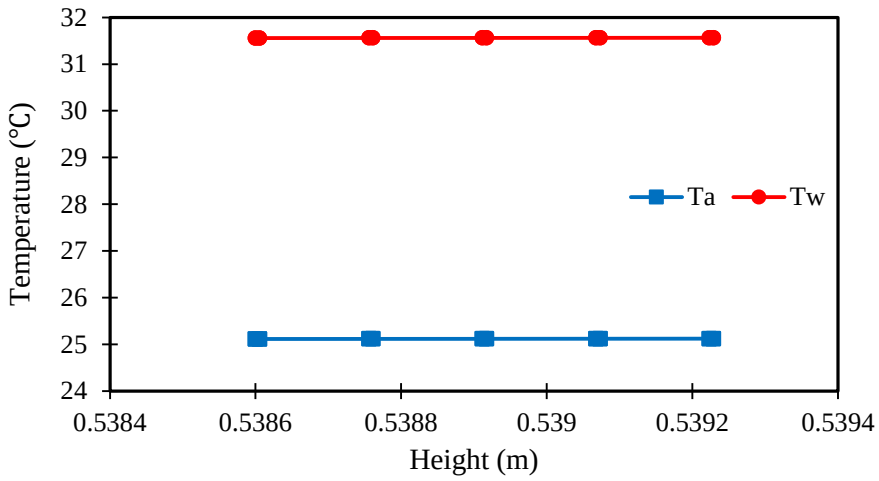

Figure 11. Supersaturated case study temperature distributions along a finite step size

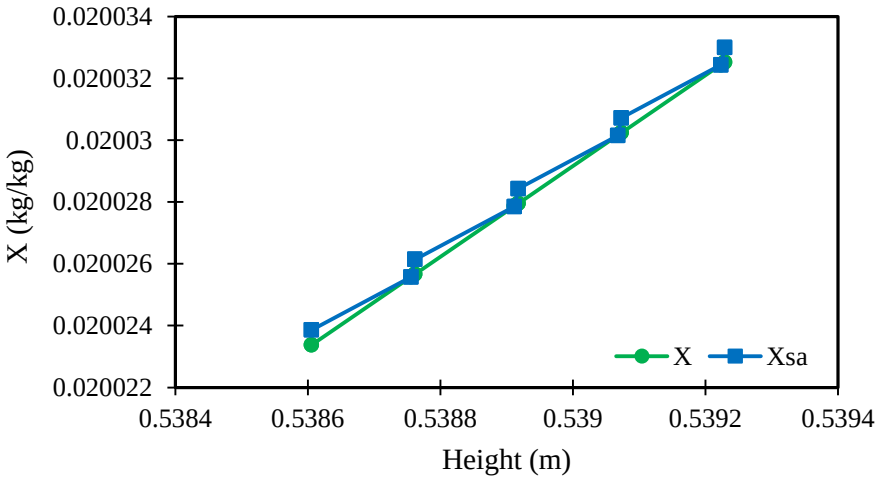

Figure 12. Supersaturated case study humidity distributions along a finite step size

2.5 Validation of full scale cooling tower

As the cooling tower results for the lab scale cooling towers were validated, it would now be possible to validate the model with a full cooling tower. The tower data was obtained from Kloppers (2003). However, Klimanek and Białecki (2009) also used this data for validating their distribution model.

Table 3. Input parameters for the full cooling tower case study

Parameter	Value
$m_{w,i}$	12500 kg/s
m_a	16672.19 kg/s
X_i	0.008127 kg/kg
T_{wi}	40.0 ℃

T_{ai}	15.45 ℃
Me	1.5548
Height (fill)	2.504 m

Figures 13 – 16 show the results obtained from the simulation. The temperature distributions shown in Figure 13 are in agreement with the results obtained from Klimanek and Białecki (2009). Discrepancies of the outlet temperatures were found to be between 2-3 ℃, which is an acceptable margin of error. However, compared to the literature results, the point of saturation was found to be at 1.7 m as opposed to 2 m. This discrepancy in results can only be attributed to the correlations used within the system as well as the gPROMS ODE solver. By reaching saturation earlier, it would have a knock on effect on the heat transfer of the system, as the rate of heat transfer would primarily be driven by sensible heat transfer than evaporative heat transfer. Other sources of error include the fact that the simulation was iteratively solved with assumed endpoint values for the water stream.

Figure 14 shows the humidity ratio distribution along the height of the cooling tower. Results found were in close agreement with simulations found in literature, as the literature results had shown that the system reached super saturation after 2 m. Whereas in the simulation, results had shown that the system had only become saturated. It can be argued that these results are valid because only certain conditions must be met before super saturation occurs. For instance, when the humidity meets the saturation humidity line, the physics would explain that more water would condense back into liquid than it evaporates. Therefore, the condensation would lower the humidity towards the saturation humidity. As this phenomenon would be very fast, it would actually be very difficult to see the system going into a supersaturated state. As literature results show that there is a degree of super saturation, the difference between the humidity ratio and the saturation humidity ratio increases. The issue is that with the physics of the system, it is known when a system is super saturated, thermodynamics would dictate that the system would only remain this way for a short while as water would condense until the system would become saturated. Although there is a difference in the physics of the simulation, actual discrepancies of the humidity ratio and saturation humidity ratio were only found to be 5-6% in comparison to Klimanek and Białecki (2009).

The mass flowrate of water within the tower was also under investigation and Figure 15 shows the results. The outlet water flowrate only had a discrepancy of 3% compared to Klimanek and Białecki (2009), which is an acceptable margin. The reason for this

discrepancy was ultimately due to the literature simulation reaching a state of super saturation, which meant that more water was being condensed and thus the results of this simulation had more water being lost to evaporation.

Figure 16 shows the Lewis factor distribution along the height of the cooling tower. In comparison to Sections 2.3 and 2.4, it can be seen that it is increasing along with the height of the cooling tower. The reason for this increase is that the zone of saturation is much higher than the previous sections and thus the rate of mass and heat transfer would increase exponentially as the humidity differential between the humidity ratio and the saturation humidity evaluated at water temperature are very close.

Upon investigation of this full cooling tower model, it can be said that this model is valid enough to be used for a parametric sensitivity analysis. Although discrepancies were found, they were not large enough to invalidate the model.

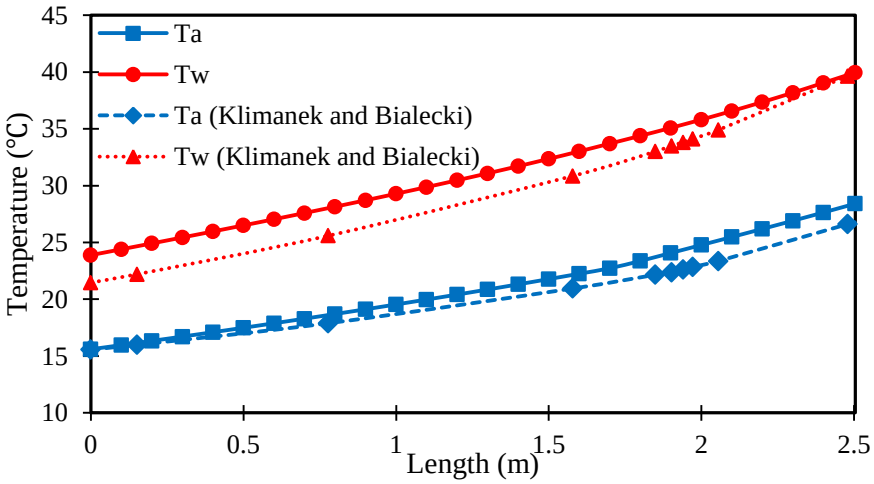

Figure 13. Temperature distribution results of full-scale cooling tower

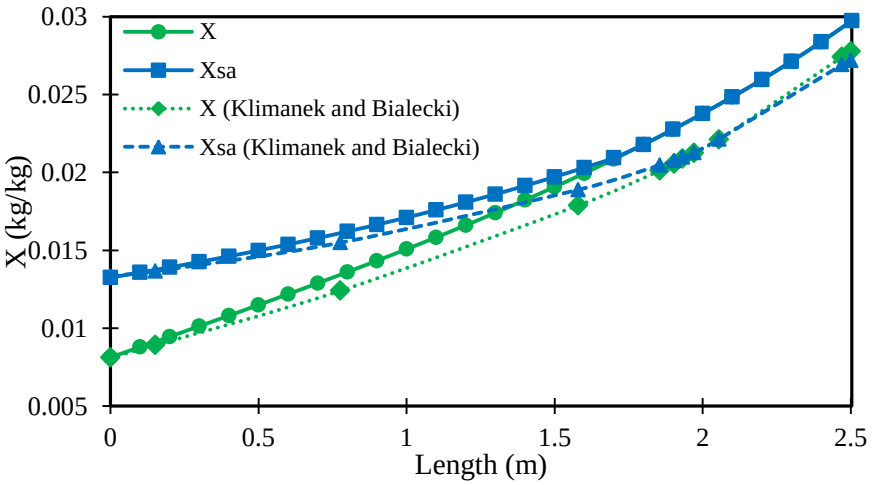

Figure 14. Humidity ratio distribution results of full-scale cooling tower

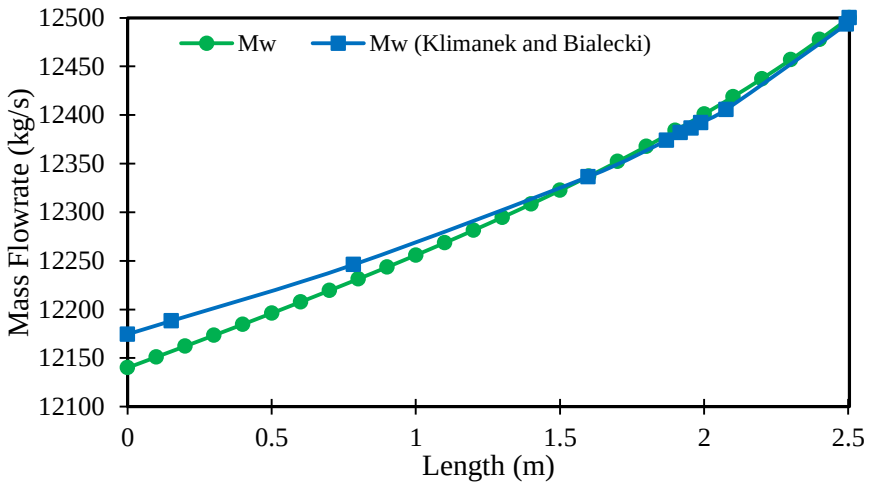

Figure 15. Water mass flowrate distribution - full-scale cooling tower

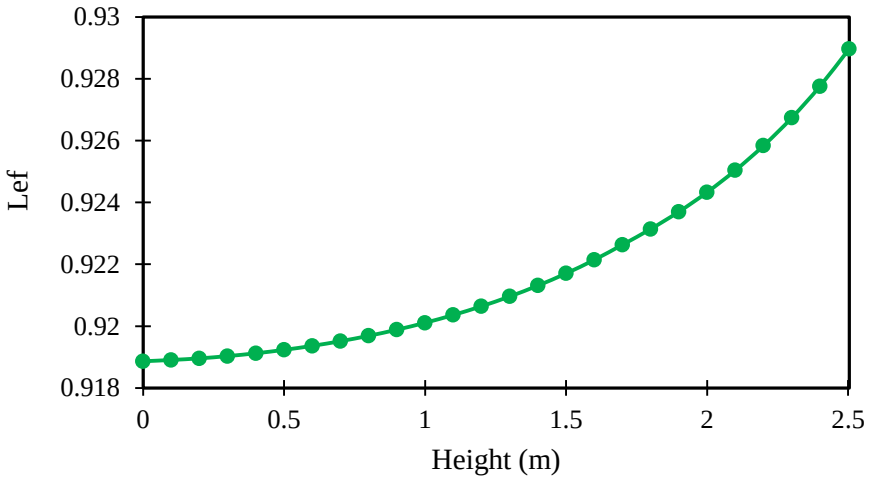

Figure 16. Lewis factor distribution - full-scale cooling tower

3. Parametric sensitivity analysis

As the mass transfer characteristic (Merkel number) is dependent on the height of the tower, the mass flowrate of air and water; an explicit expression is required to study the impact of these parameters on the tower. For the full-scale tower, this expression was obtained from Kloppers (2003). The transfer coefficient in this particular fill is written as Eq. (22) – (26).

$$Me = 0.27928 G_w^{-0.094} G_a^{0.6023} \quad (22)$$

Where G_w and G_a are expressed as:

$$G_w = \frac{m_w}{A_{fr}} \quad (23)$$

$$G_a = \frac{m_a}{A_{fr}} \quad (24)$$

The Merkel number in the rain zone is expressed as:

$$Me_{rz} = \frac{h_{drz} a_{rz} H}{G_w} \quad (25)$$

The Merkel number in the spray zone is given as:

$$Me_{sp} = 0.2 L_{sp} \left(\frac{G_a}{G_w}\right)^{0.5} \quad (26)$$

The hourly operating cost of the cooling tower was also calculated through Eq. (27) which is an adapted function obtained from Panjeshahi et al. (2009). PP is the pumping power required by the pump to deliver the water to the fill in kW and the blowdown water flowrate is obtained from Eq. (32). m_{ev} is the mass of evaporated water or the difference between inlet and outlet water flowrates in kg/s. For this work, the number of cycles of concentration was assumed to be 5 as the water was assumed to be of freshwater origin in comparison to seawater.

Operating cost = pumping cost + makeup cost + chemical treatment cost + blowdown treatment cost

$$OC = C_{PP} + C_{makeup} + C_{chemical} + C_{blowdown} \quad (27)$$

$$C_{PP} = (1.7967E-3 \times PP) \quad (28)$$

$$C_{makeup} = \left(1034.136 \times m_{makeup}\right) \quad (29)$$

$$C_{chemical} = (49.968 \times m_w) \quad (30)$$

$$C_{blowdown} = (516.96 \times m_{blowdown}) \quad (31)$$

$$m_{blowdown} = 3600 \times \frac{m_{ev}}{n_{cycle}-1} \quad (32)$$

$$m_{makeup} = m_{blowdown} + (3600 m_{ev}) \quad (33)$$

$$PP = \frac{m_w \times \rho \times g \times h}{0.85 \times 1E06} \quad (34)$$

3.1 Sensitivity of fill height

As the model itself uses the height of fill as the independent variable, a sensitivity analysis of the height of the fill will yield valuable data for a design engineer. In this study, the full-scale tower outlined in Section 2.5 will be used as the base case. For this section, the height of the fill was increased from the base case of 2.504 m to 4 m and reduced to 1 m.

Figures 17 – 20 show the results of the sensitivity analysis. It is apparent from Figure 17 that by increasing the height of the fill zone, the outlet temperature of the water had only slightly decreased by 0.69% when moving from 1 m to 2.504 m. However, when moving from 2.504 m to 4 m, the outlet temperature had decreased by 11%. Possible reasons for this occurring is down to the level of saturation and supersaturation occurring throughout the three different configurations as shown in Figure 18. At a fill height of 1 m it is possible that the high rate of heat transfer is attributed to the fact that with a smaller height, the system would reach saturation very quickly whereby the level of mass and heat transfer would increase proportionately. At the fill height of 2.504 m, the point of saturation occurs much later on which would mean that the change in convective heat and mass transfer and the rate of evaporation would not have a significant effect on the system. When the fill height was set to 4 m, there was a significant change in the system response as the system actually reached a supersaturated state. It is for this reason that the outlet temperatures were significantly the lowest as in the supersaturated state; more water was being condensed back into the liquid phase along with releasing the latent heat of vaporisation, which heated up the air stream. However, the local temperature difference between the water stream and air stream remained positive, which meant convective heat transfer was still taking place. As the air slightly heated up, the saturation humidity also increased which explains how the system had returned to a saturated state at 3.5 m.

Figure 19 shows the results of the water mass flowrates at the different fill heights. When the fill height increased from 1 m to 2.504 m, the mass of water that had evaporated had decreased by 3.22%. Possible reasons for this include the fact that with a higher length of fill, there is a greater degree of supersaturation occurring in which water vapour condenses back into the bulk water phase. It was also observed that the mass flowrate of water evaporating in the 4 m fill had increased by 19.46% compared to that of 2.504 m. Reasons for this behaviour includes the fact, as the height of the fill is significantly high, there is more area for evaporative heat transfer to occur of which the degree of condensation is proportionately similar to 2.504 m.

Figure 20 shows the results of the cost analysis. It can be seen that as the height of the fill is increased by 60% from 1 m to 2.504 m, the operating cost decreases by 3.22%. This is

because as the fill height increases, the degree of evaporation reduces due to super saturation occurring. Therefore, the water condenses from the gaseous form and thus the blowdown and water treatment costs reduce by the same proportion of 3.22%. However, when the height of the fill is further increased by 37.4% (4 m), all of the costs increase by 22.5%. The large increase in costs are attributed to the fact that as there is such a large surface area for heat transfer, the degree of evaporation is at its highest. Therefore, it is for this reason the mass flow of blowdown water and makeup water has increased in order to compensate for the larger degree of water lost due to evaporation.

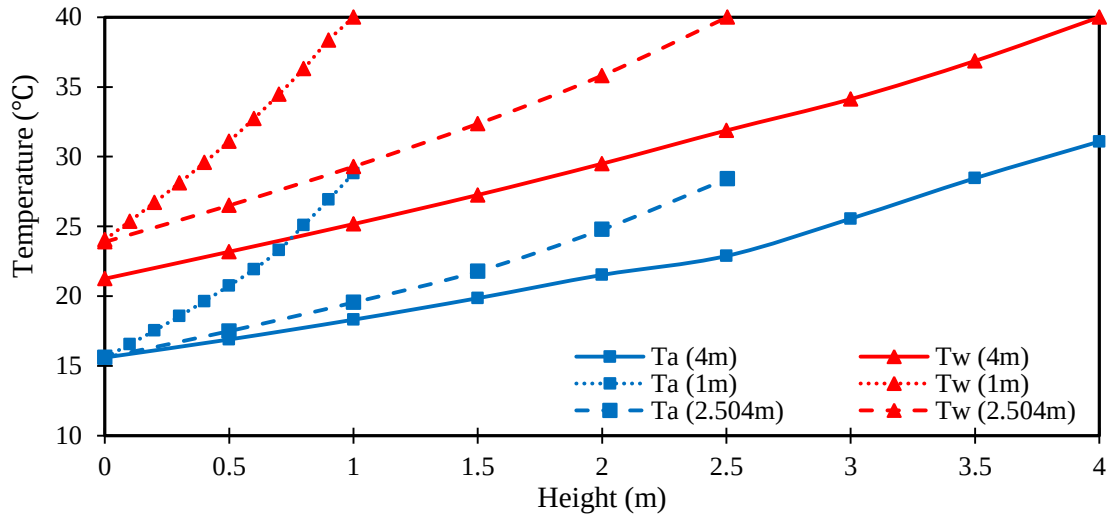

Figure 17. Sensitivity results of changing fill height - temperature distributions

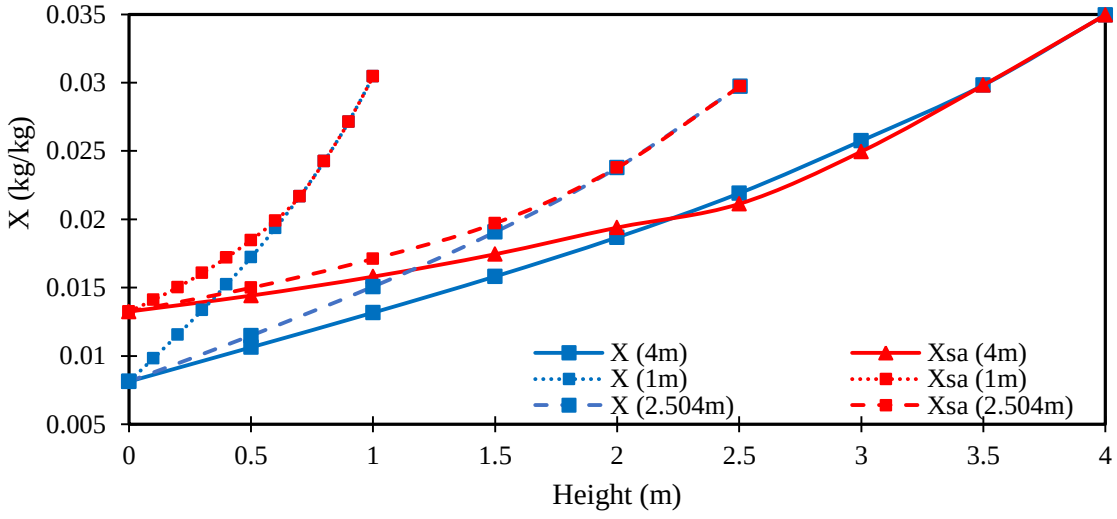

Figure 18. Sensitivity results of changing fill height – humidity ratio distributions

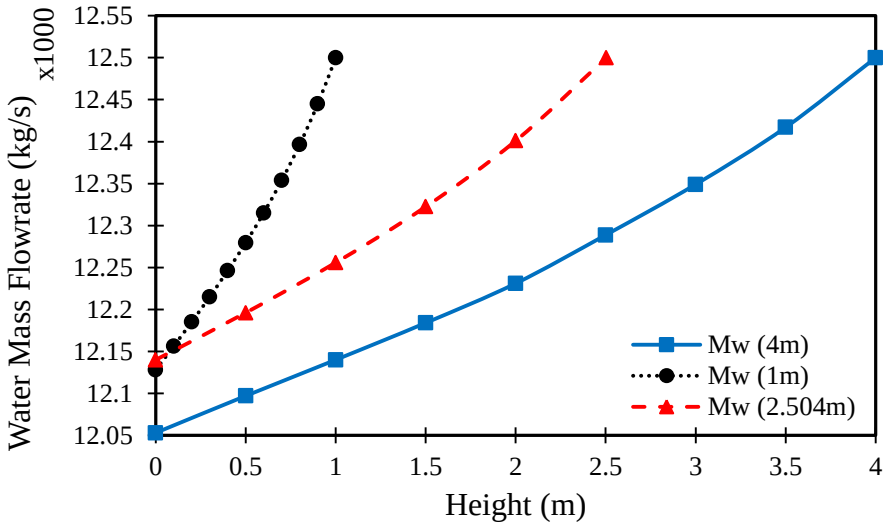

Figure 19. Sensitivity results of changing fill height - mass flowrate of water distribution

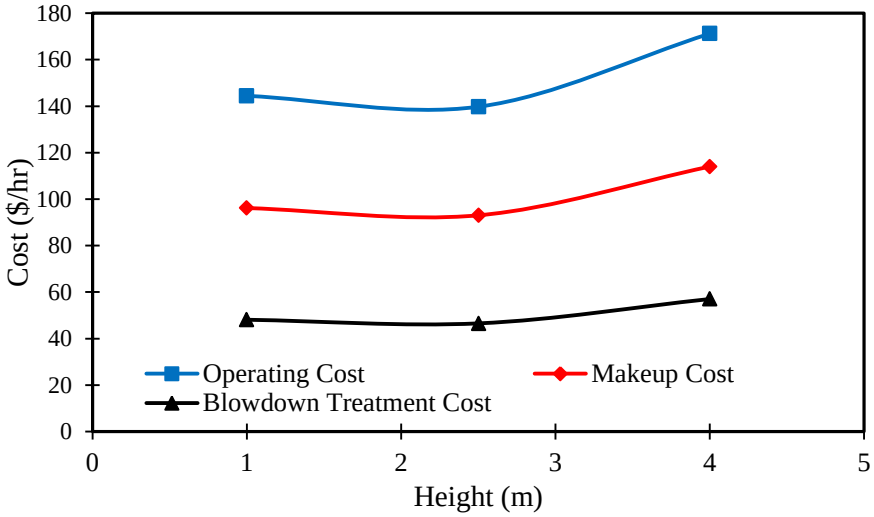

Figure 20. Sensitivity results of changing fill height – cost analysis

3.2 Sensitivity of water mass flowrate

As traditional works in literature has focused on the sensitivity of the "L/G ratio" such as by Lemouari et al. (2007) and Gharagheizi et al. (2007). This particular work will focus on treating the mass flows of water and air independently. In this section, the sensitivity of changing the mass flowrate of water will be undertaken in increments of 2500 kg/s from 1000 kg/s to 15,000 kg/s.

Figures 21-25 display the results obtained from the simulations. In Figure 21, it can be seen that despite the large changes in the mass flowrate of water, the actual outlet temperatures only range between 22.99 ℃ – 24.65 ℃. It is important to note that with higher mass flowrates of water yielded in higher outlet temperatures. This is because as the mass flow of water increases and the mass flow of air remains constant, there is less surface area for the extra

mass flow to reject the heat to the air stream. It is for this same reason that at higher flowrates of water, the temperature of the air leaving the cooling tower is also increasing despite the outlet water temperature to also increase. As the outlet water temperatures do not differ significantly, it can be said that a cooling tower is a very robust unit operation if the water flowrates do change over the design life through turndown.

Figure 22 shows the humidity distribution of the simulations. Results found were in line with expectations as with higher mass flowrates of water, the outlet humidity ratios had increased. This increase is attributed to the fact that as it is an evaporative heat transfer process, more water is being evaporated in the process from the bulk phase, as there is more water available for heat and mass transfer. Furthermore, it is also observed that the point of saturation occurs at lower heights when the mass flowrate of water increases. Reasons for this behaviour include the fact that as the mass flowrate of water increases, more water is available to be evaporated and therefore saturation would occur at an earlier point in the fill.

Figure 23 shows the distribution of the water flowrate along with the change in the mass of flowrate. An observation made is the fact that when the flowrate increased from 10,000 kg/s to 12,500 kg/s, the evaporation rate had increased by 16.11% which is a significant increase. Upon a further increase to 15,000 kg/s, the evaporation rate had increased by a further 13.67%. Possible reasons for this increase in the evaporation rate is attributed to the same reasons outlined in the previous paragraph. As the flowrate of water for heat and mass transfer has now increased, the rate of mass transfer and heat ejection would proportionately increase due to an increased heat load.

Figure 24 outlines the results obtained from the cost analysis. As the mass flowrate of water is increased by 20% from 10,000 kg/s to 12,500 kg/s, all of the costs increase by 19.20%. This is because as the mass flowrate of water increases, the degree of evaporation/condensation increases as the degree of supersaturation also increases due to an increase in mass transfer. As more liquid water evaporates from the system, the blowdown and makeup water costs increase proportionally. Upon a further increase in the mass flowrate of water by 16.67% (15,000 kg/s), all of the costs increase by 15.83%. This means that the rate of evaporation has now decreased and thus the costs affiliated with replacing lost water has also decreased. An increase from 10,000 kg/s to 12,500 kg/s (25% increase) had resulted in an increase of 25% in requirements of pumping power. However, when increasing to 15,000 kg/s (16.67%) had only yielded a 15.83% increase in the operating cost. This shows that pumps are typically most cost effective at high flowrates.

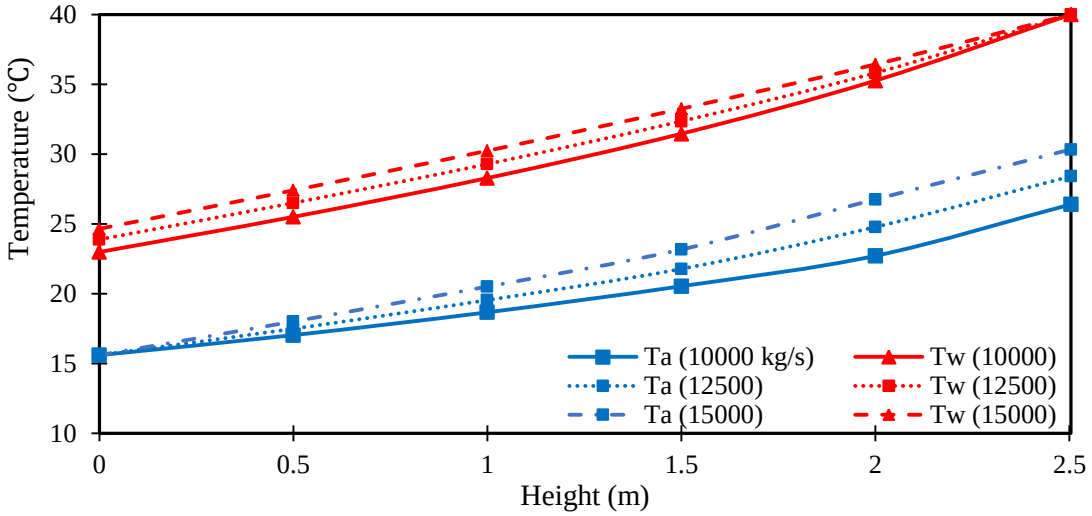

Figure 21. Sensitivity results of changing the mass flowrate of water – temperature distributions

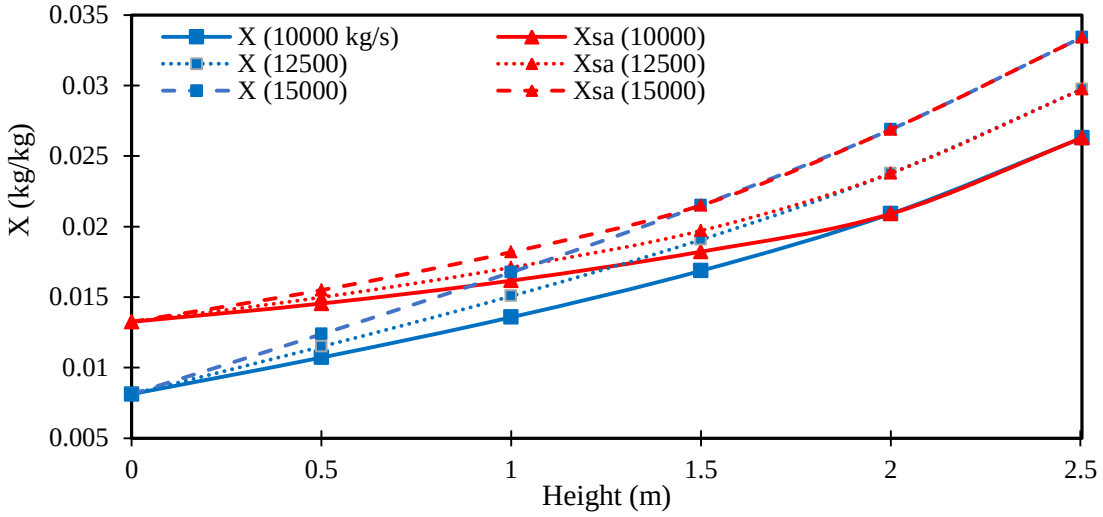

Figure 22. Sensitivity results of changing the mass flowrate of water – humidity distributions

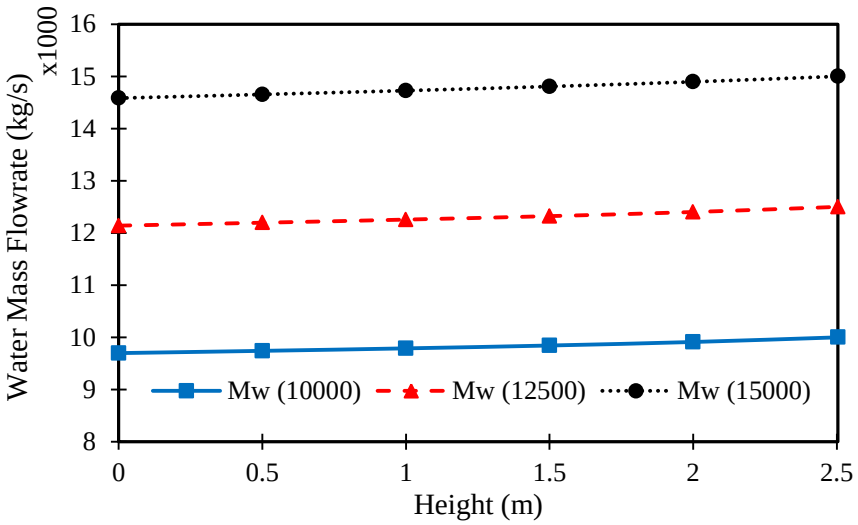

Figure 23. Sensitivity results of changing the mass flowrate of water – mass flowrate of water distributions

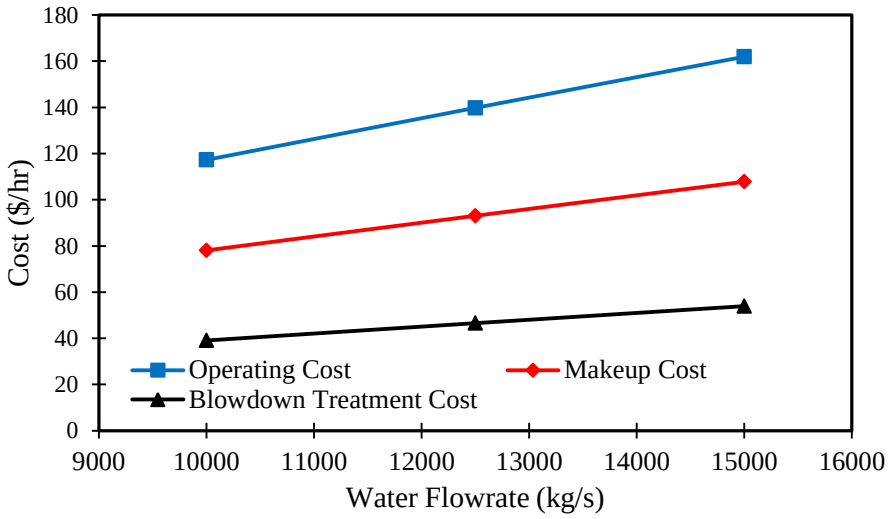

Figure 24. Sensitivity results of changing the mass flowrate of water – cost analysis

3.3 Sensitivity of air mass flowrate

The mass flowrate of air was also used for sensitivity analysis with a range of inputs between 10,000 kg/s to 15,000 kg/s. Figures 25 – 28 show these results. It can be seen in Figure 25 that the change in the mass flowrate of air has a much bigger effect on the system than changing the mass flowrate of water. The resultant outlet temperature had decreased by 12% when the mass of air had increased from 10,000 kg/s to 16,672 kg/s, which signifies a large decrease as expected. This reduction is attributed to increasing flowrate, where there is a greater mass for heat and mass transfer. This in turn would increase the rate at which heat would be ejected through sensible and evaporative heat transfer. However, it was observed that when it was increased from 16,672 kg/s to 20,000 kg/s, the outlet temperature had only reduced by 4.71%. This therefore shows that low mass flowrates of air can be detrimental to a cooling towers performance.

With respect to the outlet air temperatures, a similar observation was found whereby between 10,000 kg/s to 16672 kg/s, the air temperature had reduced by 12.8%. Between 16,672 kg/s and 20,000 kg/s, the air temperature had then only decreased by 4.2%. Reasons for this behaviour are due to the same reasons discussed before i.e. larger heat load and a larger air mass flow requires more heat rejection from the water stream in order to reach higher temperatures. Conversely, from an engineering standpoint, these results show that wind behaviour can have adverse effects on the cooling capacity of the cooling tower and as it is a natural draft cooling tower under investigation, future design considerations must

accommodate for changes in mass flow of air within the design envelope obtained from design calculations.

Figure 26 shows the humidity distributions of the sensitivity analysis. Results were in line with expectations as the mass flowrate of air increased; the humidity ratio of the air stream had decreased. The humidity ratio at the outlet had decreased by 22.26% as a result of increasing the air flowrate from 10,000 kg/s to 16,672 kg/s. Upon a further increase to 20,000 kg/s, the humidity ratio had only decreased by 7.03%. This behaviour is described by the fact that as the air flowrate increases, it provides a greater driving force for mass transfer to occur. As the water flowrate remains constant, the concentration of water in the vapour phase (humidity ratio) would actually decrease due to an increase in the air flowrate. This explains why the humidity at 10,000 kg/s is 138.38% higher than the humidity ratio at 20,000 kg/s.

As the driving force for evaporation is the difference between the actual humidity ratio and the saturation humidity ratio, it explains the difference in the mass flowrates of water as shown in Figure 27. It can be seen that as the flowrate of air increases, the evaporation rate increases (water flowrate at outlet reduces). For example, when the mass flowrate of air increases from 10,000 kg/s to 16,672 kg/s, the water flowrate at the outlet reduces by 0.48% or 58 kg/s. A further increase to 20,000 kg/s had led to a decrease in the outlet water flowrate by 0.24% or 30 kg/s. As previously mentioned, the evaporation rate is dependent on the local concentration difference between the humidity of the air and the saturation humidity, the humidity ratio in the air is a function of the mass of the air stream as a greater mass would induce a large concentration difference for mass transfer. The significance of these results is related to the fact that in the real world where the air velocity or mass flowrate is dynamic, these changes in the air flowrate can have a significant effect on the evaporation rate within the cooling tower. Such changes in the flowrate of the water leaving the fill zone must be accounted for in the design and operation of the cooling towers.

Figure 28 shows the results acquired from the cost analysis. Upon increasing the mass flowrate of air from 10,000 kg/s to 16,672 kg/s (40% increase), all of the costs had increased by 19.20%. Reasons for this includes the fact that as the mass flowrate of air increases, the degree of evaporation also increases as outlined previously. It is for this reason that the costs increase in order to replenish the water lost due to blowdown and evaporation. Upon a further increase in the mass flowrate of air by 24.22% (22,000 kg/s), all of the costs only increase by 8.33%. This large reduction in the rate of increase in costs is attributed to the fact that as water is the limiting variable, with such a large amount of air, the rate of increase in the degree of evaporation has now reduced significantly. As the driving force for evaporation is

dependent on the humidity differential, with an increase in air, the driving force for evaporation still increases although the saturation humidity ratio does not as it is temperature dependent. Therefore, it is this, which causes the operating cost to not increase at the same rate as there is a greater likelihood of condensation in the supersaturated state.

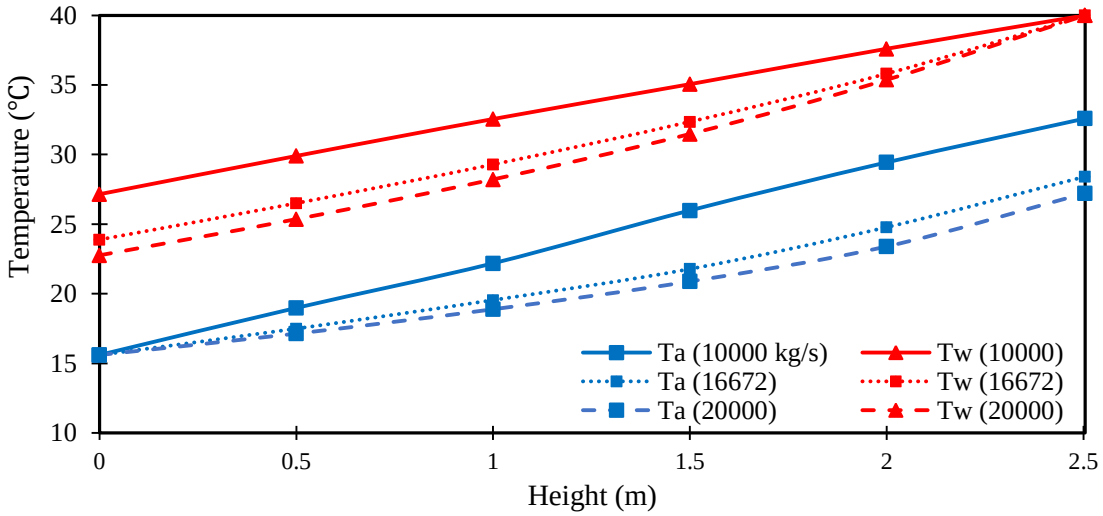

Figure 25. Sensitivity results of changing the mass flowrate of air – temperature distributions

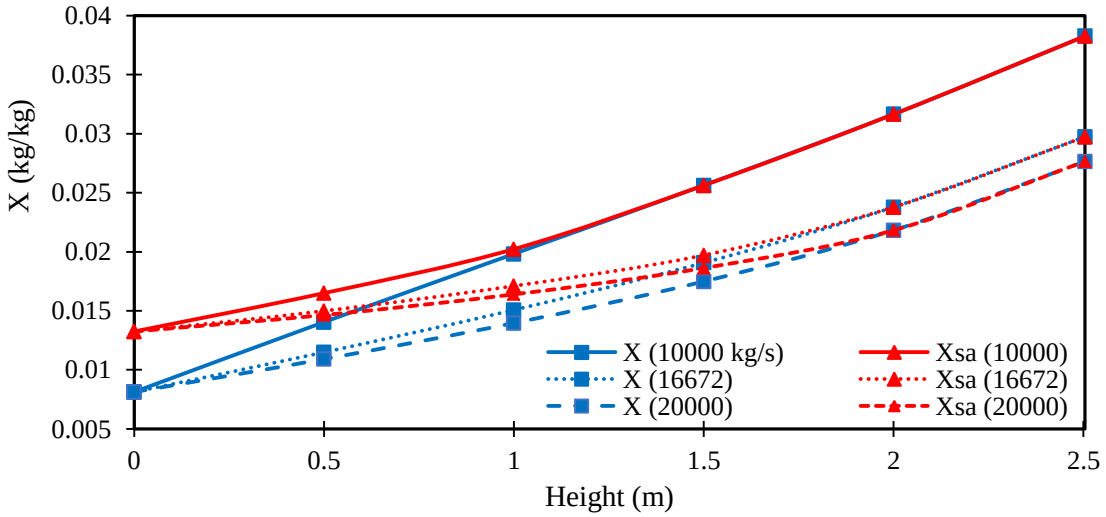

Figure 26. Sensitivity results of changing mass flowrate of air – humidity ratio distributions

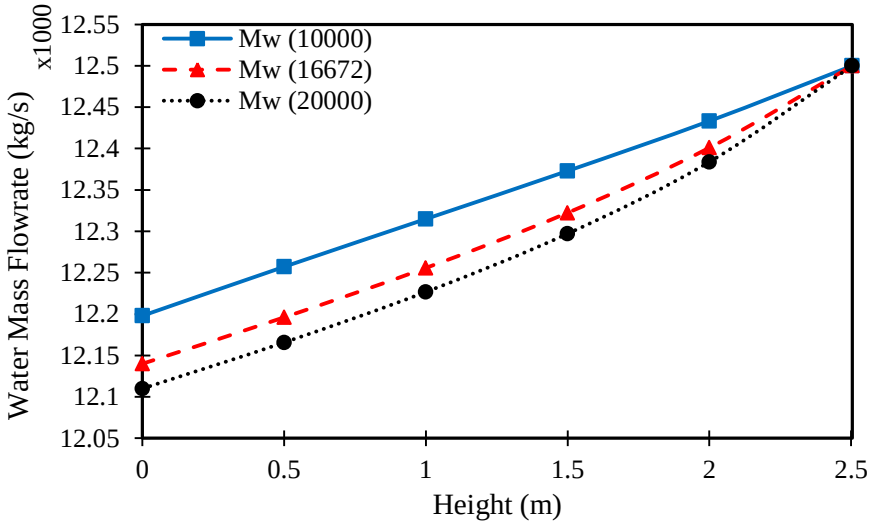

Figure 27. Sensitivity results of changing the mass flowrate of water – mass flowrate of water distributions

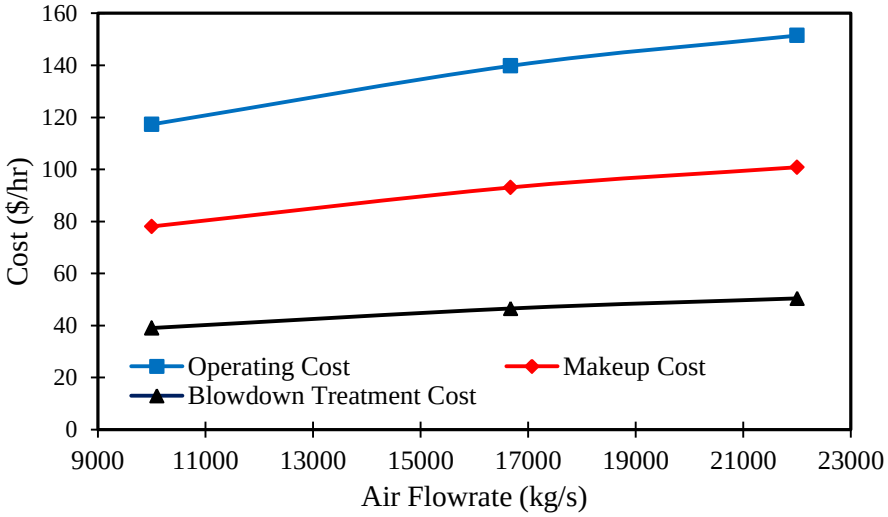

Figure 28. Sensitivity results of changing the mass flowrate of water – cost analysis

4. Conclusions

A model proposed by Klimanek (2015) was benchmarked using gPROMS with three case studies; an unsaturated system, a saturated system and a full-scale cooling tower. Results had shown good agreement with the values obtained in the literature across all three case studies and any discrepancies were down to the solver used or the thermophysical properties of air and water. Thereafter a parametric sensitivity study was undertaken in order to investigate the effects of changing such parameters on the system performance. Results from the sensitivity analysis had shown that the cooling tower is more sensitive to the change in the flowrate of air compared to a change in the flowrate of water. With a 40% increase in air flowrate, the outlet air temperature had reduced by 12.8%. However, with an increase of 54.54% in the air flowrate, the operating costs had only increased by 22.53%. With respect to the water

flowrate, an increase of 33.33% in the mass flow of water had resulted in a 27.58% increase in the operating cost. Furthermore, it was also observed that the change in the height of the fill did have major implications on the performance of the cooling tower. By selecting a large height, there is a tendency for the system to reach supersaturation, which can inhibit the performance of the cooling tower. By having a small height of fill, the issue found was that there is not enough contact time to maximise the heat transfer effectively. From a cost perspective, an increase in the fill height of 75%, the operating cost had only increased by 15.65%.

Nomenclature

a: Surface area per unit volume (m^{-1})

A_{fr}: Frontal area (m^2)

A_z: Cross sectional area of fill (m^2)

C: Fluid capacity rate (kJ/kg°C)

$C_{blowdown}$: Blowdown treatment cost ($/hr)

$C_{chemical}$: Chemical treatment cost ($/hr)

C_{makeup}: Makeup water cost ($/hr)

C_{min}: Unmixed air stream flowrate (kg/hr)

C_p: Specific heat capacity (J/kg)

C_{pp}: Cost of pumping water ($/hr)

$CDAWC$: Continuous differential air water contactor

e: Effectiveness

g: Gravity (m/s^2)

G_a: Mass flowrate of air per unit frontal area ($kg/s.m^2$)

G_w: Mass flowrate of water per unit frontal area ($kg/s.m^2$)

H: Height of tower (m)

h: Differential head of water to top of fill (m)

h_{drz}: Mass transfer coefficient (rain zone) ($kg/m^2.s$)

i_{ma}: Enthalpy of air water vapour mixture per unit mass of dry air (J/kg)

i_{masw}: Enthalpy of saturated air evaluated at water temperature (J/kg)

L_{sp}: Height of spray zone (m)

Le_f: Lewis factor

m_a: Mass flowrate of air (kg/s)

$m_{blowdown}$: Blowdown water flowrate (kg/hr)

Me_M: Merkel number from Merkel model

m_{ev}: Evaporated water flowrate (kg/s)

m_{makeup}: Makeup water flowrate (kg/s)

m_w: Mass flowrate of water (kg/s)

NTU: Number of transfer units

OC: Operating cost ($/hr)

P: Ambient pressure (Pa)

P_s: Saturation pressure (Pa)

Q: Heat exchange (kW)

r_o: Latent heat of vaporisation (J/kg)

T_a: Temperature of air (℃/K)

T_w: Temperature of water (℃/K)

w: Mass fraction dry air (kg/kg)

X: Humidity ratio (kg/kg)

X_s: Saturation humidity ratio (kg/kg)

α: Heat transfer coefficient (kW/m² s)

β: Mass transfer coefficient (kg/m² s)

ρ: Density of water (kg/m^3)

λ: Correction factor

Subscripts

i: Inlet

o: Outlet

rz: Rain zone

sp: Spray zone

sw: Saturated at water temperature

v: Water vapour

References

Berman L., 1961. *Evaporative cooling of circulating water*. New York: Pergamon Press, 90-99.

Bosnjakovic F., 1965. *Technical Thermodynamics*, Holt, Rinehart and Winston, New York.

Feltzin A., and Benton D., 1991. A More Exact Representation of Cooling Tower Theory. *The Cooling Tower Institute Journal*, 12(2), 8-26.

Gao M., Shi Y., Wang N., Zhao Y., and Sun F., 2013. Artificial neural network model research on effects of cross-wind to performance parameters of wet cooling tower based on level Froude number. *Applied Thermal Engineering*, 51(1-2), 1226-1234.

Gharagheizi F., Hayati R., and Fatemi S., 2007. Experimental study on the performance of mechanical cooling tower with two types of film packing. *Energy Conversion and Management*, 48(1), 277-280.

Hajidavalloo E., Shakeri R., and Mehrabian M., 2010. Thermal performance of cross flow cooling towers in variable wet bulb temperature. *Energy Conversion and Management*, 51(6), 1298-1303.

Jaber H. and Webb R., 1989. Design of Cooling Towers by the Effectiveness-NTU Method. *Journal of Heat Transfer*, 111(4), 837.

Jin G., Cai W., Lu L., Lee E., and Chiang A., 2007. A simplified modelling of mechanical cooling tower for control and optimization of HVAC systems. *Energy Conversion and Management*, 48(2), 355-365.

Khan J., Yaqub M., and Zubair S., 2003. Performance characteristics of counter flow wet cooling towers. *Energy Conversion and Management*, 44(13), 2073-2091.

Klimanek A., 2013. Numerical Modelling of Natural Draft Wet-Cooling Towers. *Archives of Computational Methods in Engineering*, 20(1), 61-109.

Klimanek, A., and Białecki, R., 2009. Solution of heat and mass transfer in counterflow wet-cooling tower fills. *International Communications in Heat and Mass Transfer*, 36(6), 547-553.

Kloppers J., 2003. *A critical evaluation and refinement of the performance prediction of wet-cooling towers*. PhD Thesis. University of Stellenbosch

Kloppers J., and Kroger D., 2004. A Critical Investigation into the Heat and Mass Transfer Analysis of Crossflow Wet-Cooling Towers. *Numerical Heat Transfer*, Part A: Applications, 46(8), 785-806.

Kloppers J., and Kroger D., 2005a. Cooling Tower Performance, Merkel, Poppe, A critical evaluation of Merkel assumptions. *R&D Journal SAIMechE*, 20(1), 6-10.

Kloppers J., and Kroger D., 2005b. A critical investigation into the heat and mass transfer analysis of counterflow wet-cooling towers. *International Journal of Heat and Mass Transfer*, 48(3-4), 765-777.

Kröger D., 2004. *Air-Cooled Heat Exchangers and Cooling Towers*. 1st ed. Tulsa: PennWell Corporation.

Lemouari M., Boumaza M., and Mujtaba I. M., 2007. Thermal performances investigation of a wet cooling tower. *Applied Thermal Engineering*, 27(5-6), 902-909.

Lemouari M., Boumaza M., and Kaabi A., 2009. Experimental analysis of heat and mass transfer phenomena in a direct contact evaporative cooling tower. *Energy Conversion and Management*, 50(6),1610-1617.

Llano-Restrepo M., and Monsalve-Reyes R., 2017. Modeling and simulation of counterflow wet-cooling towers and the accurate calculation and correlation of mass transfer coefficients for thermal performance prediction. *International Journal of Refrigeration*, 74, 47-72.

Martín M., and Martín, M., 2017. Cooling limitations in power plants: Optimal multiperiod design of natural draft cooling towers. *Energy*, 135, 625-636.

Merkel F., 1925. Verdunstungskuhlung. *VDI Zeitschriff Deustscher Ingenieure*, 70, 123–128.

Nasrabadi M., and Finn D., 2014. Mathematical modeling of a low temperature low approach direct cooling tower for the provision of high temperature chilled water for conditioning of building spaces. *Applied Thermal Engineering*, 64(1-2), 273-282.

Osterle F., 1991. On the analysis of counter-flow cooling towers. *International Journal of Heat and Mass Transfer*, 34(4-5), 1313-1316.

Panjeshahi M., Ataei A., Gharaie M. and Parand R., 2009. Optimum design of cooling water systems for energy and water conservation. *Chemical Engineering Research and Design*, 87(2), 200-209.

Poppe M., and Rogener H., 1991. Berechnung von ruckkuhlwerken, *VDI-Warmeatlas*, vol. 111, 1–15.

Process System Enterprise Ltd., *gPROMS Introductory User Guide*. London: Process System Enterprise Ltd., (2001).

Shah P., and Tailor N., 2015. Merkel's Method For Designing Induced Draft Cooling Tower. *International Journal of Advanced Research in Engineering and Technology*, 6(2), 63-70.

Verma P., 2004. *Cooling Water Treatment Handbook*. Albatross Fine Chem Ltd, p.82.

Yang X., Sun F., Wang K., Shi Y., and Wang N., 2007. Numerical Simulation of Flow Fields in a Natural Draft Wet-Cooling Tower. *Journal of Hydrodynamics*, Ser. B, 19(6), 762-768.

Appendix. Thermophysical properties

The following thermophysical properties used in this work was obtained from Kroger (2004). All temperatures are evaluated in degrees Kelvin.

Specific heat of dry air:

$$C_{pa} = 1.045356E3 - (3.161783E-1 \times T) + (7.083814E-4 \times T^2) - (2.705209E-7 \times T^3) \quad \text{(A.1)}$$

Saturation water vapour pressure:

$$P_s = 10^z \quad \text{(A.2)}$$

$$z = \left(\left(10.79586 * \left(1 - \left(\frac{273.16}{T}\right)\right)\right) + \left(5.02808 * LOG10\left(\frac{273.16}{T}\right)\right) + \left(0.000150474 * \left(1 - 10^{-8.29692*\left(\left(\frac{T}{273.16}\right)-1\right)}\right)\right) + \left(0.00042873 * \left(10^{4.76955*\left(1-\left(\frac{273.16}{T}\right)\right)} - 1\right)\right) + 2.786118312\right) \quad \text{(A.2)}$$

Specific heat of water vapour:

$$C_{pv} = 1.3605E3 + (2.31334 \times T) - (2.46784E-10 \times Ta^5) + (5.91332E-13 \times Ta^6) \quad \text{(A.3)}$$

Specific heat of saturated liquid water:

$$C_{pw} = 8.15599E3 - (2.80627 \times (10 \times T)) + (5.11283E-2 \times T^2) - (2.17582E-13 \times T^6) \quad \text{(A.4)}$$

Saturation humidity ratio:

$$X_s = 0.622 \times \left(\frac{P_s}{P-P_s}\right) \quad \text{(A.5)}$$